Journal of Asian Earth Sciences 110 (2015) 141–150

Contents lists available at ScienceDirect

Journal of Asian Earth Sciences

journal homepage: www.elsevier.com/locate/jseaes

U–Pb zircon geochronology, geochemistry and geodynamic significance of basaltic trachyandesites and trachyandesites from the Jianchang area, western Liaoning Province, China

GuangYing Feng [a,*], Shen Liu [b,*], CaiXia Feng [b], YuHong Yang [c], Chaogui Yang [c], Liang Tang [c], JingSui Yang [a]

[a] CARMA, State Key Laboratory of Continental Tectonics and Dynamics, Institute of Geology, Chinese Academy of Geological Sciences, Beijing 100037, China
[b] State Key Laboratory of Continental Dynamics and Department of Geology, Department of Geology, Northwest University, Xi'an 710069, China
[c] State Key Laboratory of Ore Deposit Geochemistry, Institute of Geochemistry, Chinese Academy of Sciences, Guiyang 550002, China

ARTICLE INFO

Article history:
Received 10 May 2013
Received in revised form 10 July 2014
Accepted 11 July 2014
Available online 1 August 2014

Keywords:
Basaltic trachyandesites and trachyandesites
Cretaceous
Geochronology
Sr–Nd isotopes
NCC

ABSTRACT

Basaltic trachyandesites and trachyandesites from the northern North China Craton (NCC) provide an excellent opportunity to examine the nature of their mantle source and the secular evolution of the underlying mantle lithosphere. In addition, our study of these rocks helps to constrain the age and mechanism of NCC lithospheric destruction. In this paper, we report geochronological, geochemical, and Sr–Nd isotopic analyses of the Niujiaogou (NJG) basaltic trachyandesites and trachyandesites. Laser ablation-inductively coupled plasma-mass spectrometry (LA-ICP-MS) zircon U–Pb dating yielded an age of 120.7 ± 0.8 million years, which we regard as the crystallization age of the rocks. Analysed whole-rock samples are enriched in both light rare earth elements and large ion lithophile elements (i.e. Rb, Sr and Ba), but depleted in heavy rare earth elements and high field strength elements (i.e. Nb, Ta, and Ti), with slightly negative to positive Eu anomalies (Eu/Eu^{*} = 0.73–1.09). The NJG basaltic trachyandesites and trachyandesites are characterized by low MgO (2.42–3.69 wt.%), Cr (10.3–24.6 ppm) and Ni (17.1–25.6 ppm), suggesting that they may have originated from an extremely evolved magma. In addition, the rocks display negative $\varepsilon_{Nd}(t)$ values (−12.2 to −8.5), which indicate that they were derived from a common lithosphere mantle that had previously been metasomatized by fluids related to subduction of Paleo-Asian Ocean sedimentary units. This magmatism may have been induced by large-scale, trans-tensional strike-slip on the Tan-Lu fault zone. In accord with earlier studies, these findings provide evidence that the lithospheric mantle source beneath western Liaoning Province was not changed much by the extensive Mesozoic magmatism during Triassic to early Cretaceous time.

© 2014 Elsevier Ltd. All rights reserved.

1. Introduction

The North China Craton (NCC) formed by amalgamation of the Eastern and Western Blocks at 1.85 Ga (Zhao et al., 2001, 2005), and the majority of the craton remained stable up to the Triassic; however, the eastern part of the NCC underwent extensive destruction and modification during the Mesozoic and Cenozoic (Griffin et al., 1998; Xu, 2001; Wu et al., 2005a,b, 2008; Zhai, 2008a,b; Gao et al., 2009; Zheng and Wu, 2009; Zhu and Zheng, 2009; Liu et al., 2010a). These events caused dramatic changes in the structure and nature of the NCC. In particular, the composition of the lithosphere in this area changed from old, enriched cratonic mantle to younger, depleted oceanic-type mantle (Zhou et al., 2005; Zhou, 2006). However, the mechanism, timing, range, and dynamic setting of this destruction, as well as the composition of the lithosphere prior to destruction, remain controversial (Wu et al., 2008; Zheng and Wu, 2009) due to a lack of systematic research into the geochronology, source characteristics, and evolution of mantle-derived magmatism in this area (Guo et al., 2001; Wu et al., 2003a,b, 2008; Xu et al., 2004). Mesozoic intermediate-silicic volcanic rocks are widespread along the northern margin of the NCC, western Liaoning Province. Previous research divided these rocks into four formations, from oldest to youngest; the Xinglonggou (176.6 Ma), Lanqi (166–148 Ma), Yixian (132–120 Ma), and Zhanglaogongtun (~106 Ma) Formations (Zhang et al., 2005a; Yang, 2007). These Jurassic and Cretaceous rocks provide an excellent opportunity to investigate the evolution of the underlying lithospheric mantle and the mechanism by which it was thinned (Yang and Li, 2008). These rift-related, Mesozoic volcanic rocks

* Corresponding authors. Tel.: +86 18611245102 (G. Feng), +86 18092512436 (S. Liu).
E-mail addresses: fengguangying198@163.com (G. Feng), liushen@nwu.edu.cn (S. Liu).

http://dx.doi.org/10.1016/j.jseaes.2014.07.025
1367-9120/© 2014 Elsevier Ltd. All rights reserved.

are predominantly basaltic trachyandesites to trachyandesites or trachydacites that can potentially provide invaluable information concerning continental extension in the region (Hall, 1982; Li et al., 1997; Liu et al., 2004; Liu et al., 2006a,b; Windley, 1984; Zhou et al., 1998). The present study focuses on the Niujiaogou (NJG) basaltic trachyandesites and trachyandesites of the Jianchang area of western Liaoning Province. Zircons from these rocks yielded a U–Pb age of 120 ± 0.8 Ma, consistent with the age of the Yixian Formation (132–120 Ma; Yang, 2007) and with the most extensive and intense magmatism in the eastern NCC. Previous Sr–Nd–Pb isotope analyses of mafic rocks (mainly basalt and gabbro) suggested that the lithospheric mantle in this area was isotopically heterogeneous and had a special spatial and temporal distribution (Xu et al., 2004; Zhai et al., 2004; Zhang et al., 2004; Zhou et al., 2005), although these studies mainly focused on the Luxi, Jiaodong, and Taihang Mountain regions. The present study discusses the properties of the Mesozoic lithospheric mantle beneath the northern NCC, and aims to improve our understanding of the evolution of the lithospheric mantle and to constrain the timing and mechanism involved in thinning of the NCC lithosphere.

2. Geological background and petrography of the volcanic rocks

The western area of Liaoning Province lies along the northern margin of the NCC (Fig. 1) and is bounded by an Archean craton to the south and the Paleozoic Xingmeng Orogenic Belt (XMOB) to the north. The NCC is one of the oldest Archean cratons in the world, with ages extending back to 3.8 Ga (Liu et al., 1992; Zhao and Cawood, 2012; Zhao and Zhai, 2013). The cratonization of the NCC occurred in the Early Paleoproterozoic at ~1.85 Ga (Zhao, 2001; Wilde et al., 2002; Kroner et al., 2006; Liu et al., 2006a,b), and the area was covered by thick sedimentary deposits during the Middle-Late Proterozoic and the Paleozoic (Chen and Chen, 1997). The NCC is cut by the Tan-Lu fault zone, a strike-slip fault that was initiated between the Jurassic and the Early Cretaceous (Zhu et al., 2001a); this tectonism led to deformation and graben formation in the area during the late Cretaceous and Tertiary (Zhu et al., 2001b).

The XMOB was formed through collision of the NCC and Siberian plates, and is composed of several blocks and/or terranes, namely the northernmost Erguna Massif, the central Xing'an, Songliao, and Liaoyuan terranes and the eastern Jiamusi Block and the Raohe Complex. The amalgamation of northeast China occurred predominantly during the Paleozoic and Mesozoic; the Erguna Massif collided with the Xing'an terrane in the early Paleozoic, whereas collisions between the Xing'an, Songliao, and Liaoyuan terranes occurred in the late Paleozoic (Zhou et al., 2009, 2010a,b,c, 2011; Wilde et al., 2010). Later accretion of the Jiamusi massif to the Songliao terrane occurred between the Early and Late Jurassic; this was followed by Late Jurassic-Early Cretaceous accretion of the Raohe complex (Wu et al., 2011).

The western part of Liaoning Province lies within the northern margin of the NCC and is on the western side of the Tan-Lu fault zone. This area is part of the eastern Yanshan zone, and is underlain by cratonic Precambrian basement. This old cratonic basement was formed during the Lüliang movement in the Neoarchean, and then underwent a long and stable development stage, followed by intense tectonism and magmatism in the Mesozoic, when the NCC was in an intraplate orogenic stage of development. The early Mesozoic tectonic evolution of this area was controlled by the Paleo-Asian tectonic domain, whereas it was constrained by the Pacific tectonic domain during the Middle-Late Mesozoic (Ma and Zheng, 2009; Wu et al., 2000; Zhang, 2006).

The study area is located in the Jianchang basin (Fig. 1b), in western Liaoning Province. Exposed units in the area include basaltic trachyandesites, trachyandesites, and pyroclastic rocks of the Tiaojishan Group, all of which have similar compositions; andesites, conglomerates, and sandy conglomerates of the Yaolugou Group; rhyolites and trachytes of the Early Cretaceous Yixian Formation; and sandy conglomerates, silty shales and rhyolites of the Late Cretaceous Yixian Formation (Fig. 1b). The basaltic trachyandesite and trachyandesites sampled during this study were intruded into the Yixian Formation. These rocks are grey-black in color, medium-grained, massive with a diabasic texture. The studied samples obtained during this study generally contain 25–30 vol% of medium-grained (0.5–1.5 mm) plagioclase and minor pyroxene microphenocrysts. Some of the plagioclase are moderately to strongly altered.

3. Analytical methods

3.1. LA-ICP-MS U–Pb dating

Zircons were separated from one > 40-kg rock sample (NJG2-01) using conventional heavy liquid and magnetic techniques at

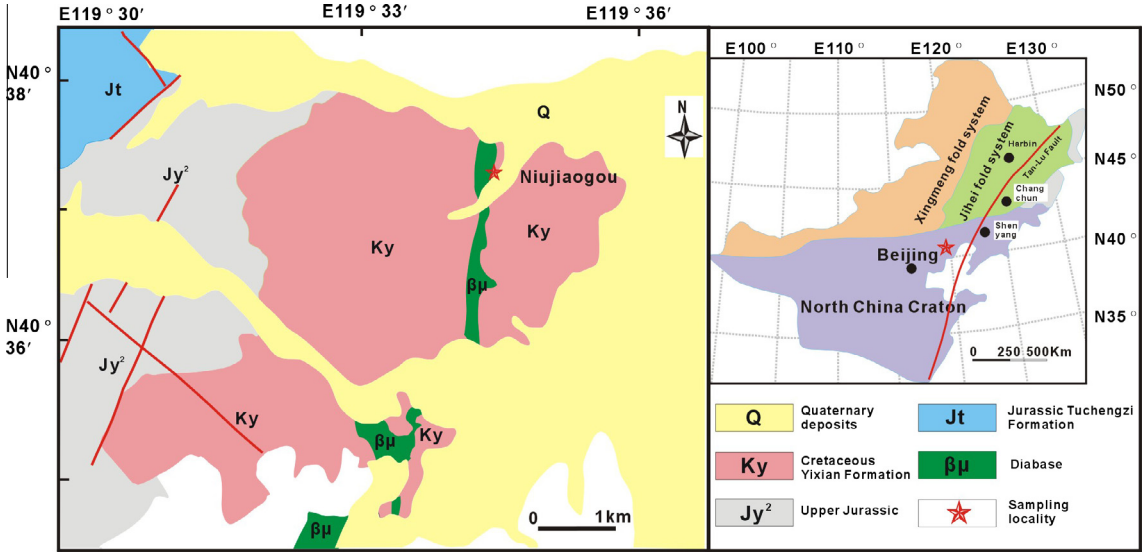

Fig. 1. Geological map of the study area, including the locations of samples of the Niujiaogou basaltic trachyandesites and trachyandesites taken during this study.

the Langfang Regional Geological Survey, Hebei Province, China. Representative zircons were hand-picked under a binocular microscope and mounted in an epoxy resin disc, before polishing and gold coating. Zircons were imaged under transmitted and reflected light and cathodoluminescence (CL) at the State Key Laboratory of Continental Dynamics, Northwest University, China to determine their external and internal structures.

Zircons were U–Pb dated using LA-ICP-MS at the State Key Laboratory of Geological Processes and Mineral Resources, China University of Geosciences, Wuhan, using the laser ablation and ICP-MS conditions and data reduction techniques outlined in Liu et al. (2008a, 2010b, 2010c). An Agilent Chemstation was utilized for the acquisition of each individual analysis, off-line selection, and integration of background and analyte signals, and ICPMSDataCal (Liu et al., 2008a, 2010c) was used for time-drift correction and quantitative calibration during both trace element and U–Pb analysis.

Zircon 91500 was used as an external standard during U–Pb dating, and was analyzed twice for every five analyses of unknowns. Time-dependent drift of U–Th–Pb isotopic ratios was corrected using a linear interpolation (with time) and with drift corrections calculated and applied every five analyses according to variations in the 91500 zircon analysis (i.e., one correction every two zircon 91500 + five unknown samples + two zircon 91500 analyses; Liu et al., 2010c). The U–Th–Pb isotopic ratios for the 91500 standard used during this study are those of Wiedenbeck et al. (1995). The uncertainties on these preferred 91500 values were propagated through to the overall uncertainties for each zircon analysis, and concordia diagrams and weighted mean calculations were undertaken using Isoplot/Ex ver3 (Ludwig, 2003).

3.2. Whole-rock geochemical analysis

The major and trace element of 15 representative samples were determined during this study. Prior to analysis, whole-rock samples were trimmed to remove altered surfaces, and were cleaned with deionized water before crushing and subsequent powdering in an agate mill.

Major element concentrations were determined using a PANalytical Axios-advance (Axios PW4400) X-ray fluorescence (XRF) spectrometer at the State Key Laboratory of Ore Deposit Geochemistry, Institute of Geochemistry, Chinese Academy of Sciences (IGCAS), Guiyang. Analysis was undertaken on fused glass discs, and the analytical precision, as determined using Chinese National standard GSR-3, was better than 2%. Loss on ignition (LOI) values was determined using 1 g of powder, heated to 1100 °C for 1 h.

Trace element concentrations were determined using a Perkin–Elmer Sciex ELAN 6000 ICP-MS instrument at IGCAS. Each analysis used 50 mg of powdered sample, which was dissolved using a HF + HNO_3 mixture for 48 h at ca. 190 °C in high-pressure Teflon bombs (Qi and Conrad, 2000). Rh was used as an internal standard during analysis to monitor signal drift, and the GBPG-1 international standard was used for analytical quality control. The analytical precision during ICP-MS was generally better than 5% for all elements and analyses of the OU-6 and GBPG-1 international standards are in agreement with recommended values.

3.3. Sr–Nd isotope analyses

Whole-rock Sr–Nd isotopic data were obtained using a Finnigan Triton multi-collector mass spectrometer at the State Key Laboratory of GPMR. Sr and Nd isotopic fractionation was corrected to $^{86}Sr/^{88}Sr = 0.1194$ and $^{146}Nd/^{144}Nd = 0.7219$, respectively. Analysis of the NBS987 and La Jolla standards yielded average values of $^{87}Sr/^{86}Sr = 0.710215 \pm 10$ and $^{143}Nd/^{144}Nd = 0.511837 \pm 1$, respectively (both 2σ), and total procedural Sr and Nd blanks of <4 and <1 ng, respectively. Details of the analytical approach are given in Zhang et al. (2004).

4. Results

4.1. Zircon U–Pb dating

Sufficient zircons were selected from basaltic trachyandesite sample NJG2-01 for U–Pb analysis during this study. These zircons are euhedral, colorless, transparent, mostly elongate and prismatic, ranging up to 100 μm in diameter. The majority of zircons have oscillatory or planar zoning in CL images (Fig. 2), a typical feature of magmatic zircons. The zircons have variable Th (62.1–758 ppm) and U (127–956 ppm) concentrations, yielding Th/U ratios of 0.45–0.80 (Table 1), providing additional evidence of a magmatic origin. Zircon U–Pb dates for these samples are given in Table 1, Eighteen analyses on 18 oscillatory-zoned grains yielded concordant dates and a weighted mean $^{206}Pb/^{238}U$ age of 120.7 ± 0.8 Ma (Fig. 2). This age is interpreted as the crystallization age of the basaltic trachyandesites and trachyandesites in the study area.

4.2. Major and trace elements

The analysed whole-rock samples were variably altered with LOI ranging from 3.01 to 5.62 wt.% and an average of 4.66 wt.% (Table 2). Al_2O_3, TiO_2, CaO and P_2O_5 concentrations do not vary with LOI values, whereas Fe_2O_3, MgO and Na_2O concentrations increase slightly and SiO_2 concentrations decrease with increasing LOI. In addition, generally mobile elements, such as Rb, Sr and Ba, show moderate degrees of scatter. Given this, we focus the following discussion on the REE and the high field strength elements (i.e. Nb, Ta, Ti) and Y, Al, P and Ca (cf., Arndt et al., 1998; Song et al., 2008).

The major element concentrations of the analyzed samples are given in Table 2. All of the analyses were normalized to 100% volatile-free before plotting on classification diagrams. These rocks have SiO_2 contents of 52.42 to 57.72 wt.%, and all they have relatively high total alkalies ($Na_2O + K_2O = 8.23–9.68$ wt.%). In the TAS diagram they plot in the fields of basaltic trachyandesite and trachyandesite (Fig. 3). All of the samples have low MgO concentrations (2.57–3.82 wt.%; $Mg^{\#} = 43–50$) and show negative correlations between MgO and SiO_2, K_2O, Cr, and Zr, and positive correlations between MgO and Al_2O_3, P_2O_5, TiO_2, Fe_2O_3, and

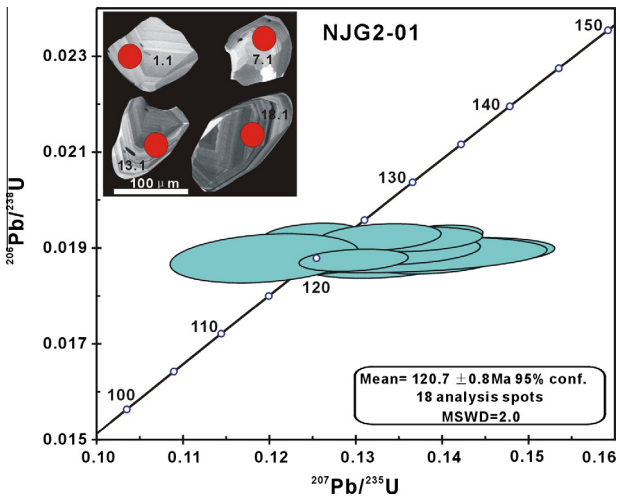

Fig. 2. Representative cathodoluminescence images and LA-ICP-MS U–Pb concordia diagrams for zircons obtained from basaltic trachyandesite sample NJG2-01.

Table 1
LA-ICP-MS U–Pb isotope data for zircons separated from sample Niujiaogou basaltic trachyandesite sample NJG2-01.

Grain	Element concentrations				Isotopic ratios						Age (Ma)					
	Th (ppm)	U (ppm)	Pb (ppm)	Th/U	$^{207}Pb/^{206}Pb$	1s	$^{207}Pb/^{235}U$	1s	$^{206}Pb/^{238}U$	1s	$^{207}Pb/^{206}Pb$	1s	$^{207}Pb/^{235}U$	1s	$^{206}Pb/^{238}U$	1s
1	235	292	16.5	0.80	0.0525	0.0031	0.1328	0.0075	0.0187	0.0003	307	103	127	7	119	2
2	195	328	15.8	0.59	0.0489	0.0021	0.1248	0.0052	0.0186	0.0002	145	80	119	5	119	1
3	62.1	137	5.53	0.45	0.0548	0.0027	0.1390	0.0067	0.0188	0.0003	402	83	132	6	120	2
4	163	306	13.2	0.53	0.0476	0.0021	0.1220	0.0052	0.0187	0.0002	78	77	117	5	119	1
5	423	651	32.3	0.65	0.0493	0.0013	0.1280	0.0034	0.0188	0.0001	161	48	122	3	120	1
6	126	220	9.96	0.57	0.0531	0.0022	0.1382	0.0056	0.0189	0.0002	334	73	131	5	121	1
7	438	583	32.8	0.75	0.0490	0.0014	0.1271	0.0036	0.0188	0.0002	150	50	122	3	120	1
8	79.6	146	6.71	0.54	0.0543	0.0037	0.1414	0.0095	0.0189	0.0003	381	158	134	8	121	2
9	758	956	53.1	0.79	0.0467	0.0014	0.1202	0.0036	0.0186	0.0001	34	51	115	3	119	1
10	170	293	13.6	0.58	0.0472	0.0018	0.1247	0.0047	0.0192	0.0002	57	63	119	4	123	1
11	94.8	127	7.79	0.74	0.0519	0.0055	0.1350	0.0140	0.0189	0.0003	282	240	129	13	120	2
12	88.6	139	7.11	0.64	0.0528	0.0031	0.1353	0.0074	0.0190	0.0003	320	100	129	7	121	2
13	346	595	28.1	0.58	0.0508	0.0018	0.1341	0.0048	0.0191	0.0002	231	65	128	4	122	1
14	341	533	27.5	0.64	0.0526	0.0016	0.1397	0.0041	0.0193	0.0002	313	50	133	4	123	1
15	153	230	12.1	0.66	0.0519	0.0024	0.1368	0.0063	0.0192	0.0002	281	87	130	6	122	1
16	155	267	12.3	0.58	0.0507	0.0023	0.1327	0.0058	0.0192	0.0002	226	80	126	5	123	1
17	94.1	167	8.22	0.56	0.0461	0.0036	0.1193	0.0090	0.0188	0.0004		172	114	8	120	3
18	198	336	16.0	0.59	0.0503	0.0020	0.1296	0.0052	0.0187	0.0002	207	74	124	5	120	1

Notes: Errors are given at 1s uncertainty, and common Pb corrections used the method of Andersen (2002).

Na_2O. In contrast, CaO, Ni, and Sr concentrations show no correlation with MgO (Fig. 4).

Trace element compositions of analyzed samples are given in Table 3. Total rare earth element (REE) concentrations range from 94.0 to 148 ppm. All samples are characterized by relatively flat heavy rare earth elements (HREE) and significant enrichment in light rare earth elements (LREE)), with $(La/Yb)_N$ values of 7.7–26.6. The samples show slightly negative to slightly positive Eu anomalies ($Eu/Eu^* = 0.73–1.09$; Fig. 5a), and they contain low concentrations of Cr (10.3–24.6 ppm), Co (25.4–42.3 ppm), and Ni (17.1–25.6 ppm), consistent with their low MgO contents. In addition, they have positive Rb, Sr, and Ba, and negative Nb, Ta, and Ti anomalies on the primitive mantle normalized multi-element diagram (Sun and McDonough, 1989; Fig. 5b).

4.3. Sr–Nd isotope data

The whole-rock Sr and Nd isotope compositions of representative basaltic trachyandesite and trachyandesite samples are given in (Table 4). These samples have very uniform $^{87}Sr/^{86}Sr$ ratios (0.7058–0.7069), and initial $^{87}Sr/^{86}Sr$ values of 0.70536–0.70546. In addition, these samples have similarly uniform Nd isotope compositions, and low initial $^{143}Nd/^{144}Nd$ (0.51186–0.51205) and $\varepsilon_{Nd}(t)$ (−12.2 to −8.5) values. All of these samples plot within the EMI enriched mantle field in a $(^{87}Sr/^{86}Sr)_i$ vs. $\varepsilon_{Nd}(t)$ diagram (Fig. 6), similar to basalts from the Yixian Formation that have $(^{87}Sr/^{86}Sr)_i$ values of 0.706144–0.706287 and εNd (t) values of −12.0 to −9.7 (Yang, 2007).

Nd isotopic model ages (T_{DM}) can be derived from the Nd isotope characteristics of rock samples. However, it is generally agreed that differing degrees of Sm/Nd fractionation mean that model ages are only valid and geologically significant in systems with $f_{Sm/Nd}$ values of −0.5 to −0.2 (Wu et al., 1997). The studied samples have Nd isotopic model ages from 1.59 to 1.81 Ga, and corresponding $f_{Sm/Nd}$ values of −0.47 and −0.43, except for sample NJG2–01, which has a value of 0.53. These data indicate that the aforementioned Paleo- to Meso-proterozoic model ages are geologically significant. Previous geochemical research on magmatic rocks and deep mantle xenoliths indicates that the lithospheric mantle beneath the NCC was enriched between the Paleozoic and the Mesozoic (Wang et al., 1996; Yan et al., 2000; Zhou et al., 2001).

5. Discussion

5.1. Fractional crystallization

The basaltic trachyandesite and trachyandesites were derived from a highly fractionated magma or low degrees of partial melting of an enriched source, as evidenced by their low MgO concentrations (2.57–3.82 wt.%; $Mg^{\#} = 43–50$, Cr (10.3–24.69 ppm) and Ni (17.1–25.6 ppm) (Liu et al., 2008b). The positive correlation between MgO and Al_2O_3, P_2O_5, TiO_2, Fe_2O_3, and Na_2O indicates that minor plagioclase, apatite, Fe–Ti oxides (rutile, ilmenite and sphene) were involved in their fractional crystallization history. Ni shows very little change with MgO and Cr increases as MgO decreases suggesting little fractionation of olivine and pyroxene. Weak negative Eu anomalies of some samples suggest minor removal of plagioclase. SiO_2 shows two distinct groups with different trends, possibly suggesting magma mixing or significant crustal contamination.

5.2. Crustal contamination and fluid metasomatism

Mantle-derived magmas can undergo crustal contamination during ascent (Mohr, 1987), and the geochemical characteristics

Table 2
Major element compositions (in wt.%) of the NJG basaltic trachyandesites and trachyandesites in western Liaoning Province.

Sample No.	SiO_2	TiO_2	Al_2O_3	Fe_2O_3	MgO	CaO	Na_2O	K_2O	MnO	P_2O_5	Total	LOI	Mg#	$Na_2O + K_2O$
NJG-01	54.59	1.13	16.79	8.59	3.56	6.37	5.72	3.02	0.12	0.11	100.00	4.58	48.00	8.73
NJG-03	57.72	1.22	16.21	7.38	3.05	5.31	5.61	3.32	0.10	0.07	99.99	5.61	48.00	8.94
NJG-02	56.08	1.25	15.99	7.68	3.02	5.89	5.08	3.95	0.11	0.06	99.11	4.82	46.00	9.03
NJG-04	56.92	1.27	15.63	7.66	3.07	5.66	3.89	5.77	0.10	0.03	100.00	5.47	47.00	9.66
NJG-05	57.58	1.20	15.61	7.43	2.62	5.69	4.08	5.60	0.11	0.04	99.96	5.55	44.00	9.68
NJG-06	57.33	1.20	16.21	7.45	2.57	5.46	4.20	5.42	0.10	0.04	99.98	5.34	43.00	9.62
NJG-07	57.02	1.34	15.89	7.80	2.72	6.07	5.26	3.55	0.11	0.05	99.81	5.62	43.00	8.81
NJG-08	56.50	1.29	16.03	7.80	3.09	5.96	4.95	4.24	0.11	0.05	100.02	4.93	47.00	9.19
NJG-09	55.31	1.42	16.57	8.71	3.62	5.73	6.01	2.21	0.10	0.31	99.99	4.15	48.00	8.23
NJG-10	54.65	1.50	16.71	8.55	3.40	6.45	5.96	2.54	0.12	0.10	99.98	4.50	47.00	8.50
NJG-11	53.29	1.45	16.31	8.25	3.41	8.03	5.60	2.99	0.14	0.51	99.98	4.19	48.00	8.59
NJG-12	54.67	1.50	16.73	8.51	3.77	5.95	6.08	2.41	0.12	0.25	99.99	4.23	49.00	8.50
NJG-13	52.42	1.38	16.08	7.53	3.44	10.04	5.77	2.85	0.15	0.33	99.99	3.01	50.00	8.63
NJG-14	54.65	1.56	16.51	8.76	3.74	5.92	6.02	2.34	0.12	0.39	100.01	4.57	48.00	8.36
NJG-15	55.29	1.55	16.49	8.65	3.82	5.30	5.55	2.99	0.09	0.28	100.01	3.37	49.00	8.54
GSR3(RV*)	45.72	2.43	14.16	13.72	7.96	9.02	3.46	2.38	0.17	0.97	99.99	2.24		
GSR3(MV*)	45.83	2.40	14.27	13.69	7.92	8.95	3.47	2.34	0.17	0.97	100.01	2.24		
GSR1(RV*)	73.63	0.29	13.55	2.16	0.42	1.57	3.16	5.06	0.06	0.09	99.99	0.70		
GSR1(MV*)	73.73	0.29	13.57	2.15	0.41	1.51	3.15	5.04	0.06	0.09	100.00	0.56		

Notes: LOI = loss on ignition, Mg# = 100 × Mg/(Mg + Fe) atomic ratio, RV* = recommended values, and MV* = measured values; values for GSR-1 and GSR-3 are from Wang et al. (2003).

of the Niujiaogou basaltic trachyandesites and trachyandesites suggest some slight crustal contamination. However, significant crustal contamination of the parental magmas is ruled out by the relatively low and uniform $^{87}Sr/^{86}Sr$ ratios.

The Mesozoic evolution of western Liaoning Province was influenced by the Paleo-Pacific tectonic regime, suggesting that the northern NCC may have been metasomatized by fluids derived from dehydration of subducted ocean crust. Previous research on high-K arc magmatism in east China suggested that it was related to subduction of the Paleo-Pacific plate beneath eastern China (Wu, 1985). However, this model has a number of inconsistencies and problems (Shao et al., 2001): (1) Mesozoic magmatism in eastern China does not have a subduction-related polarity; (2) the area of Mesozoic magmatism extends more than 1000 km into the continental interior, suggesting an extremely low-angle subduction that exceeds the geological confidence level (Zhao et al., 1998) and has no modern analogue; (3) there is no tectonic evidence of this subduction in eastern China (Miyashiro, 1973); and (4) the tectonism related to the Paleo-Pacific plate in eastern China was dominantly strike-slip rather than true subduction (Maruyama and Seno, 1986; Maruyama et al., 1997). All of this evidence suggests that Mesozoic subduction of Paleo-Pacific Ocean crust was not responsible for the magmatism in eastern China discussed here (Liu et al., 2002).

Based on the above discussion, we suggest that the magmas that formed the basaltic trachyandesites and trachyandesites were generated from a region of mantle that was metasomatized by fluids derived from dehydration of subducted Paleo-Asian Ocean crust. Even though this ocean closed in the late Paleozoic, the characteristics of the mantle were preserved for a significant post-collisional period that recorded gradual formation of new mantle source regions (Liu et al., 2002).

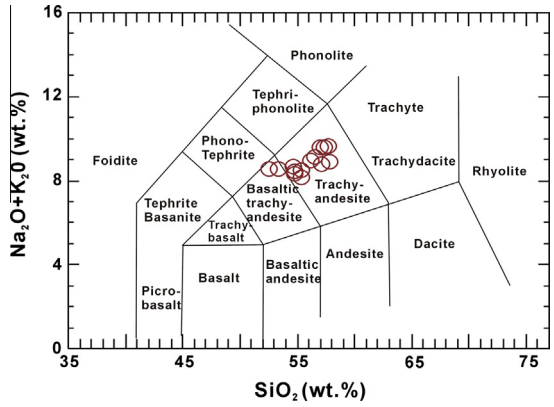

Fig. 3. Total alkali vs. silica diagrams for the Niujiaogou basaltic trachyandesites and trachyandesites samples analyzed during this study (LeMaitre et al., 1989).

5.3. Source regions

Changes in lithospheric thickness can be determined by variations in the Nd isotope values of basaltic rocks that formed during differing time periods (DePaolo and Daley, 2000), primarily because experimental results indicate that, in plume-free environments, alkali basalt magmas are generated at greater depths (>80 km) than tholeiitic magmas (50–60 km). Thus, alkali basalt magmas with enriched lithospheric mantle isotope signatures may have been generated at lithospheric depths of >80 km. The basaltic trachyandesites and trachyandesites studied here are characterized by high $Na_2O + K_2O$ concentrations (8.23–9.68 wt.%) and enriched isotope compositions ($(^{87}Sr/^{86}Sr)_i$ = 0.70536–0.70546, $^{143}Nd/^{144}Nd$ = 0.51186–0.51205, and $\varepsilon Nd_{(t)} = -12.2$ to -8.5), indicating genesis at a lithospheric depth of >80 km.

All of the analysed basaltic trachyandesites and trachyandesites plot in the same field as samples from the Yixian Formation in a $(^{87}Sr/^{86}Sr)_i$ vs. $\varepsilon_{Nd}(t)$ diagram (Fig. 6). Previous research indicates that the majority of the Yixian volcanic rocks formed at 132–120 Ma (Yang, 2007); the later stages of this magmatism may have been contemporaneous with (120.7 ± 0.8 Ma). This suggests that the Niujiaogou volcanic rocks and those of the Yixian Formation may have formed during the same magmatic event. The existence of voluminous high-Mg andesite and adakite rocks within the Yixian Formation suggests that they formed from magmas generated by partial melting of the delaminated lower crust. One potential dynamic mechanism that may have induced these magmatic events is large-scale strike-slip movements along the Tan-Lu fault zone (Yang, 2007; Yang and Li, 2008).

5.4. Petrogenesis

The Tan-Lu fault zone is a major wrench fault in northeastern Asia that extends from Nikolayevsk in Russia to the Yangtze Craton in South China, with a strike length of more than 5000 km (Xu

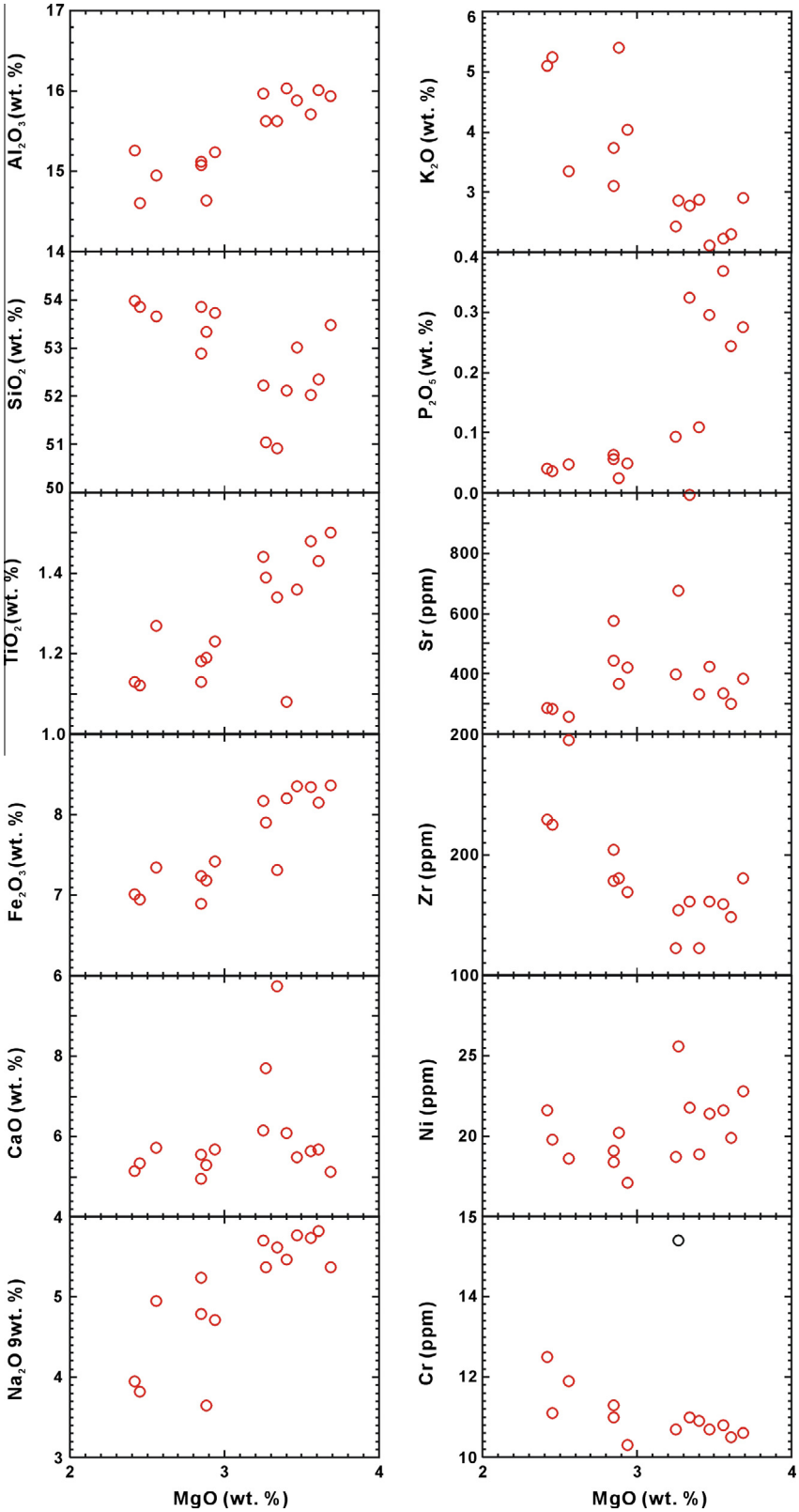

Fig. 4. Selected major and trace element variation diagrams plotted against MgO concentrations for the whole-rock samples analyzed during this study.

et al., 1987, 1993; Zheng et al., 1998). This fault cuts through the eastern part of the NCC, and previous studies (Fan and Hooper, 1989; Peng et al., 1986; Xu et al., 1993, 1996; Zheng et al., 1998, 2007) have shown that it extends deep into the lithospheric mantle. The Tan-Lu fault zone locally formed transtensional segments that led to magmatic activity, and as such may have played an important role in the evolution of the sub-continental lithospheric mantle (Xiao et al., 2010).

Geochronological research has indicated that strike-slip movement along the Tan-Lu fault may have continued until 114 Ma

Table 3
Trace elements (ppm) for Niujiaogou basaltic trachyandesites and trachyandesites from western Liaoning Province.

Sample No.	NJG-01	NJG-02	NJG-03	NJG-04	NJG-05	NJG-06	NJG-07	NJG-08	NJG-09	NJG-10	NJG-11	NJG-12	NJG-13	NJG-14	NJG-15
Sc	15.6	13.7	13.9	13.0	13.4	13.7	15.0	13.0	16.2	14.1	18.1	17.3	16.1	17.5	17.0
V	176	127	136	127	124	123	129	130	152	152	151	156	135	158	144
Cr	10.9	11.3	11.0	24.6	11.1	12.5	11.9	10.3	10.7	10.7	15.4	10.5	11.0	10.8	10.6
Co	26.7	26.9	26.7	28.3	28.1	29.5	27.9	25.4	42.3	30.0	29.2	32.4	32.3	33.5	28.0
Ni	18.9	19.1	18.4	20.2	19.8	21.6	18.6	17.1	21.4	18.7	25.6	19.9	21.8	21.6	22.8
Cu	23.5	20.1	20.3	20.0	20.1	21.1	20.4	20.0	23.2	23.1	23.6	23.9	23.1	25.1	22.6
Zn	84.1	94.1	90.6	92.3	88.8	89.5	89.8	90.6	84.8	89.0	86.2	89.0	81.3	91.6	85.4
Ga	17.3	18.2	18.4	19.6	18.1	18.8	18.5	17.5	16.9	17.6	17.4	17.9	15.8	18.4	17.7
Rb	44.6	63.2	72.8	86.5	91.0	90.8	71.7	68.4	41.5	44.1	47.2	44.1	48.1	45.1	43.1
Sr	332	577	445	366	283	286	258	421	425	397	676	302	995	335	385
Y	8.98	15.8	19.5	20.7	19.6	19.9	25.2	17.8	15.2	13.7	18.3	17.2	23.1	26.6	10.7
Zr	122	204	178	180	225	229	295	169	161	122	154	148	161	159	180
Nb	9.73	16.3	16.2	17.3	16.0	17.0	17.0	15.9	11.3	11.4	11.8	12.1	11.0	12.4	12.9
Ba	316	336	318	373	399	415	300	302	338	285	1280	319	890	398	352
La	28.9	25.5	30.2	30.6	28.7	28.5	30.1	28.9	21.2	26.4	23.8	25.8	28.1	30.1	20.3
Ce	51.9	46.9	57.8	58.2	54.8	55.8	54.9	54.4	41.0	52.5	45.4	47.7	55.1	58.0	40.1
Pr	5.34	5.08	6.56	6.69	6.21	6.45	6.15	5.93	4.86	6.22	5.15	5.28	6.80	6.87	4.43
Nd	18.4	18.5	26.0	26.1	24.3	24.6	22.8	22.8	18.6	25.6	20.8	20.1	28.7	28.6	16.9
Sm	2.81	3.45	4.82	4.61	4.64	4.58	4.17	4.11	3.22	4.65	3.57	3.07	5.38	5.43	2.98
Eu	0.90	0.83	1.24	1.22	1.19	1.17	1.08	1.06	1.05	1.68	1.18	0.95	1.82	1.96	0.91
Gd	2.61	3.37	4.72	4.64	4.41	4.56	4.59	3.98	3.13	4.69	3.80	3.05	5.83	5.95	2.61
Tb	0.35	0.48	0.69	0.67	0.66	0.66	0.75	0.56	0.44	0.63	0.55	0.44	0.76	0.89	0.37
Dy	1.76	2.81	3.57	3.62	3.48	3.56	4.39	3.18	2.50	2.87	3.09	2.72	4.15	4.54	1.98
Ho	0.35	0.60	0.77	0.80	0.77	0.77	0.98	0.67	0.52	0.55	0.71	0.63	0.87	0.93	0.40
Er	0.924	1.80	2.03	2.24	2.04	2.19	2.47	1.79	1.51	1.51	2.00	1.76	2.22	2.41	1.23
Tm	0.13	0.26	0.26	0.30	0.28	0.31	0.35	0.25	0.23	0.17	0.30	0.25	0.24	0.32	0.19
Yb	0.78	1.68	1.77	1.83	1.76	1.91	2.06	1.65	1.50	0.93	2.22	1.53	1.54	1.76	1.40
Lu	0.11	0.25	0.27	0.26	0.29	0.29	0.32	0.23	0.20	0.13	0.35	0.21	0.24	0.27	0.22
Hf	3.54	4.46	4.33	4.64	3.92	4.24	4.62	4.33	3.19	2.94	3.13	3.16	2.94	3.19	3.45
Ta	0.65	1.07	0.99	0.97	0.93	0.96	0.98	0.90	0.62	0.61	0.58	0.63	0.61	0.63	0.62
Pb	6.32	10.27	9.17	10.07	9.54	10.58	9.53	8.71	7.37	6.67	6.48	6.62	6.28	6.85	6.08
Th	1.69	3.30	3.29	2.62	2.70	2.83	2.36	2.76	3.58	1.83	3.45	3.43	4.77	6.34	1.99
U	0.32	1.36	0.70	0.56	0.64	0.69	0.92	0.62	0.95	0.14	0.96	0.78	0.49	0.97	0.57
ΣREE	115	112	141	142	134	135	135	130	100	129	113	113	142	148	94.0
La_N/Yb_N	26.6	10.9	12.2	12.0	11.7	10.7	10.5	12.6	10.1	20.4	7.7	12.1	13.1	12.3	10.4
δEu	0.99	0.73	0.79	0.80	0.79	0.77	0.75	0.79	1.00	1.09	0.97	0.94	0.99	1.05	0.98

Notes: RV* = recommended values, MV* = measured values; values for GBPG-1 and OU-6 are from Thompson et al. (2000) and Potts and Kane, 2005, respectively.

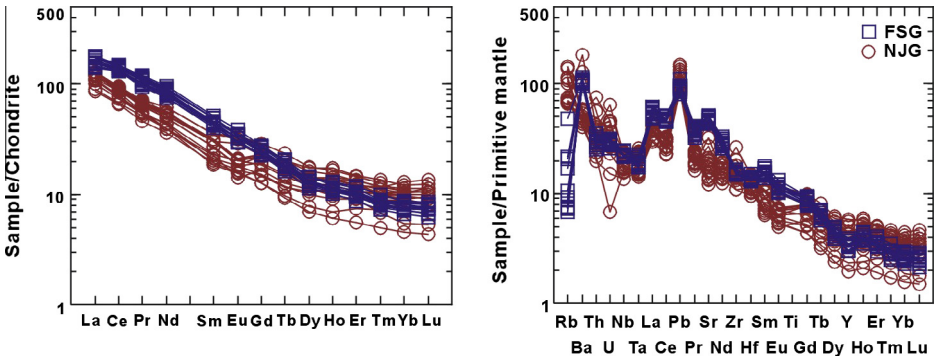

Fig. 5. Chondrite-normalized REE and primitive-mantle-normalized multi-element diagrams for the Niujiaogou basaltic trachyandesites and trachyandesites compared with samples of Fangshengou (FSG) basaltic lavas from western Liaoning Province. Normalizing values are from Sun and McDonough (1989).

Table 4
Sr-Nd isotopic compositions of the NJG basaltic trachyandesites and trachyandesites in western Liaoning Province.

Sample No.	Rb (ppm)	Sr (ppm)	$^{87}Rb/^{86}Sr$	$^{87}Sr/^{86}Sr$	±2σ	$(^{87}Sr/^{86}Sr)_i$	Sm (ppm)	Nd (ppm)	$^{147}Sm/^{144}Nd$	$^{143}Nd/^{144}Nd$	±2σ	$(^{143}Nd/^{144}Nd)_i$	ε_{Nd} (t)	T_{DM1} (Ga)	$f_{Sm/Nd}$
NJG-01	44.6	332	0.3886	0.70612	10	0.705459	2.81	18.4	0.092316	0.512121	11	0.512049	-8.5	1.29	-0.53
NJG-03	72.8	445	0.4732	0.706190	10	0.705383	4.82	26.0	0.112058	0.511966	12	0.511878	-12	1.77	-0.43
NJG-06	90.8	286	0.9185	0.70692	10	0.705356	4.58	24.6	0.112538	0.511948	12	0.511860	-12	1.81	-0.43
NJG-11	47.2	676	0.2020	0.70575	10	0.705409	3.57	20.8	0.103748	0.512004	11	0.511923	-11	1.59	-0.47

Notes: Chondrite Uniform Reservoir (CHUR) values ($^{87}Rb/^{86}Sr = 0.0847$, $^{87}Sr/^{86}Sr = 0.7045$, $^{147}Sm/^{144}Nd = 0.1967$, $^{143}Nd/^{144}Nd = 0.512638$) were used during isotoperatio calculations as follows: $\lambda_{Rb} = 1.42 \times 10^{-11}$ yr^{-1} (Steiger and Jäger, 1977); $\lambda_{Sm} = 6.54 \times 10^{-12}$ yr^{-1} (Lugmair and Harti, 1978).

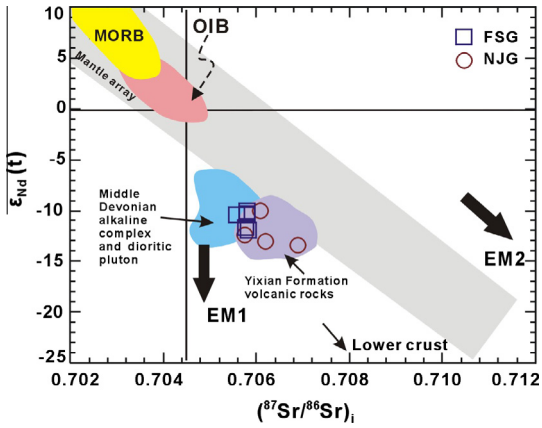

Fig. 6. Initial $^{87}Sr/^{86}Sr$ vs. $\varepsilon Nd_{(t)}$ diagram for the Niujiaogou basaltic trachyandesites and trachyandesites. Sr–Nd isotope compositions of the Middle Devonian Shuiquangou alkaline complex and the dioritic Gushan pluton are from Jiang (2005) and Zhang et al. (2007), and Yixian Formation volcanic rock Sr-Nd isotopic compositions are from Yang (2007). MORB and OIB compositions are from Zhang et al. (2002) and references therein, the mantle array lines are from Zhang et al. (2005b), and the lower crust trend is after Jahn et al. (1999).

(Niu, 2001; Zhu et al., 2001a, 2001b), at which time a change in the tectonic regime, related to high-angle orthogonal subduction of the western Pacific Plate, caused E-W-extension and a change in the stress state of the Tan-Lu fault from compression to extension. This large-scale extensional activity also caused thinning (to <80 km) of the NCC lithosphere (Yang, 2007).

These data suggest that the Niujiaogou alkaline basaltic trachyandesites and trachyandesites were genetically related to large-scale, transtensional, strike-slip movement at 135–120 Ma along the Tan-Lu fault. This movement resulted in the formation of a NNE-trending tensile basin, and upwelling of the asthenospheric mantle. This deep movement along the fault led to delamination of the thickened lithosphere near the fault belt and rapid upwelling of the decompressed asthenospheric mantle. The high heat flow caused by the upwelling asthenosphere triggered partial melting of the enriched upper mantle, which was metasomatized by fluids liberated during subduction of the Paleo-Asian Plate. Around 120 Ma, these magmas ascended along the faults, undergoing fractional crystallization of apatite, Ti-bearing minerals (e.g., rutile, ilmenite, and sphene) and minor plagioclase, before being emplaced in the upper crust, to form the Niujiaogou basaltic trachyandesites and trachyandesites.

5.5. Geological significance

Numerous studies of Mesozoic volcanic and mafic–ultramafic intrusive rocks have determined that major lithospheric thinning of the NCC took place around 120–130 Ma. However, the majority of the magmatic rocks in this period were derived from enriched lithospheric mantle material, and only limited asthenospheric mantle-derived magmatism took place at this time, suggesting that the NCC lithosphere was thicker at 120–130 Ma than it is now (Wu et al., 2003a,b). Additional studies have shown that asthenospheric mantle-derived basaltic rocks appeared in Fuxin, Liaoning Province at ~110 Ma (Zhang et al., 2003), and that mantle peridotite xenoliths carried in these rocks have the same characteristics as the mantle peridotite xenoliths in Cenozoic basalts of Eastern North China (Zheng et al., 2007). This suggests that lithospheric thinning in western Liaoning Province may have ceased before 110 Ma. Detailed studies on Mesozoic volcanic rocks from western Liaoning Province have identified four magmatic events; these events formed the Xinglonggou (176 Ma), Lanqi (166–148 Ma), Yixian (132–120 Ma), and Zhanglaogongtun (~106 Ma) Formations. Given this, we suggest that significant lithospheric thinning occurred at 120–110 Ma in western Liaoning Province, and that such thinning may have continued to as late as 106 Ma.

The Triassic (223.3 ± 1.1 Ma; Feng et al., 2012) Fangshengou basalts and the Cretaceous (120.7 ± 0.8 Ma) Niujiaogou basaltic trachyandesites and trachyandesites of western Liaoning Province have similar REE patterns and trace element characteristics (Fig. 5), and nearly identical Nd isotope signatures (Fig. 6). This means that the mantle region from which both parental magmas were sourced remained constant between the Triassic and the Cretaceous. This is consistent with the observation that the majority of volcanic rocks in western Liaoning Province have intermediate-silicic compositions. Thus, in turn suggests that the mantle sources for magmatism within the northern NCC changed only slightly over a long period until delamination resulted in significant thinning of the lithospheric mantle.

6. Conclusions

The geochronological, geochemical, and Sr-Nd isotope data presented here allow us to reach the following conclusions:

(1) Zircon U–Pb dating indicates that the Niujiaogou basaltic trachyandesites and trachyandesites were formed at 120.7 ± 0.8 Ma; these rocks formed from magmas associated with deep movements along the Tan-Lu fault.
(2) The geochemical data presented here suggest that the basaltic trachyandesites and trachyandesites were derived from a common source area of within the lithospheric mantle. This region of the mantle was metasomatized by fluids derived from entrained Paleo-Asian Ocean sediment that were subducted beneath the NCC mantle lithosphere. The parental melts of these rocks underwent variable degrees of crystal fractionation but were not contaminated by crustal material.
(3) The extensive Mesozoic magmatism in western Liaoning Province did not change the composition of the lithospheric mantle. The mantle source region for magmatism within the northern NCC changed abruptly between 120 and 106 Ma due to delamination of the lower crust resulting in significant lithospheric thinning beneath the NCC.

Acknowledgements

This study was financially supported by the Basic Outlay of Scientific Research Work from the Ministry of Science and Technology (J1321) and the National Nature Science Foundation of China (41303019 and 41373028) and grants from Sinoprobe-05-02 of the Ministry of Science and Technology of China. We are grateful to Lian Zhou for assistance with the Sr and Nd isotope analyses, and to Yongsheng Liu and Zhaochu Hu for assistance during the zircon U–Pb dating.

References

Andersen, T., 2002. Correction of common lead in U–Pb analyses that do not report ^{204}Pb. Chem. Geol. 192, 59–79.
Arndt, N.T., Chauvel, C., Czamanske, G., Fedorenko, V., 1998. Two mantle sources, two plumbing systems: tholeiitic and alkaline magmatism of the Meymecha River Basin, Siberian flood volcanic province. Contrib. Mineral. Petrol. 133, 297–313.
Chen, Y.X., Chen, W.J., 1997. Chronology, geochemistry and setting of Mesozoic volcanic rocks in West Liaoning and adjacent regions: Beijing. Seismol. Press, 141–201 (in Chinese with English abstract).
Depaolo, D.J., Daley, E.E., 2000. Neodymium isotopes in basalts of the southwest basin and range and lithospheric thinning during continental extension. Chem. Geol. 169, 157–185.

Fan, Q.C., Hooper, P.R., 1989. The mineral chemistry of ultramafic xenoliths of eastern China: implications for upper mantle composition and the paleogeotherms. J. Petrol. 30, 1117–1158.
Feng, G.Y., Liu, S., Zhong, H., Feng, C.X., Coulson, I.M., Qi, Y.Q., Yang, Y.H., Yang, C.G., 2012. U–Pb zircon geochronology, geochemical, and Sr–Nd isotopic constraints on the age and origin of basaltic porphyries from western Liaoning Province, China. Int. Geol. Rev. 54, 1052–1070.
Gao, S., Zhang, J.F., Xu, W.L., Liu, Y.S., 2009. Delamination and destruction of the North China Craton. Chin. Sci. Bull. 54, 3367–3378.
Griffin, W.L., Zhang, A., O'Reilly, S.Y., Ryan, C.G., 1998. Phanerozoic evolution of the lithosphere beneath the Sino-Korean Craton. In: Flower, M.F.J., Chung, S.L., Lo, C.H., Lee, T.Y. (Eds.), Mantle Dynamics and Plate Interaction in East Asia, vol. 27. Geodynamics Series, pp. 107–126.
Guo, F., Fan, W.M., Wang, Y.J., Lin, G., 2001. Late Mesozoic mafic intrusive complexes in North China Block: constraints on the nature of subcontinental lithospheric mantle. Phys. Chem. Earth (A) 26, 759–771.
Hall, H.C., 1982. The importance and potential of mafic dyke swarms in studies of geodynamic process. Geosci. Can. 9, 145–154.
Jahn, B.M., Wu, F.Y., Luo, C.H., 1999. Crust–mantle interaction induced by deep subduction of the continental crust: Geochemical and Sr–Nd isotopic evidence from post-collisional mafic–ultramafic intrusion of the northern Dabie Complex, central China. Chem. Geol. 157, 119–146.
Jiang, N., 2005. Petrology and geochemistry of the Shuiquangou syenitic complex, northern margin of the North China Craton. J. Geol. Soc. London 162, 203–215.
Kroner, A., Wilde, S.A., Zhao, G.C., O'Brien, P.J., Sun, M., Liu, D.Y., Wan, Y.S., Liu, S.W., Guo, J.H., 2006. Zircon geochronology and metamorphic evolution of mafic dykes in the Hengshan Complex of northern China: Evidence for late Palaeoproterozoic extension and subsequent high-pressure metamorphism in the North China Craton. Precambrian Res. 146, 45–67.
LeMaitre, R.W., Bateman, P., Dudek, A., Keller, J., Lemeyre, J., Le Bas, M.J., Sabine, P.A., Schmid, R., Sorensen, H., Steckeisen, A., Wooley, A.R., Zanettin, B., 1989. A Classification of Igneous Rocks and a Glossary of Terms. Blackwell Scientific, Oxford, United Kingdom, pp. 193.
Li, J.H., He, W.Y., Qian, X.L., 1997. Genetic mechanism and tectonic setting of a Proterozoic mafic dyke swarm: its implication for Paleoplate reconstruction. Geol. J. Chin. Univ. 3, 272–280.
Liu, D.Y., Nutman, A.P., Compston, W., Wu, J.S., Shen, Q.H., 1992. Remnants of ≥3800 Ma crust in the Chinese part of the Sino-Korean craton. Geology 20, 339–342.
Liu, H.T., Zhai, M.G., Liu, J.M., Sun, S.H., 2002. The Mesozoic granitoids in the northern marginal region of North China Craton: evolution from post-collisional to anorogenic settings. Acta Petrol. Sinica 18, 433–448.
Liu, S., Hu, R.Z., Zhao, J.H., Feng, C.X., 2004. K–Ar geochronology of Mesozoic mafic dikes in Shandong Province, Eastern China: implications for crustal extension. Acta Geol. Sinica 78, 1207–1213.
Liu, S., Zou, H.B., Hu, R.Z., Zhao, J.H., Feng, C.X., 2006a. Mesozoic mafic dikes from the Shandong Peninsula, North China Craton: petrogenesis and tectonic implications. Geochem. J. 40, 181–195.
Liu, S.W., Zhao, G.C., Wilde, S.A., Shu, G.M., Sun, M., Li, Q.G., Tian, W., Zhang, J., 2006b. Th–U–Pb monazite geochronology of the Lüliang and Wutai Complexes: constraints on the tectonothermal evolution of the Trans-North China Orogen. Precambrian Res. 148, 205–225.
Liu, Y.S., Hu, Z.C., Gao, S., Günther, D., Xu, J., Gao, C.G., Chen, H.H., 2008a. In situ analysis of major and trace elements of anhydrous minerals by LA-ICP-MS without applying an internal standard. Chem. Geol. 257, 34–43.
Liu, S., Hu, R.Z., Gao, S., Feng, C.X., Qi, L., Zhong, H., Xiao, T.F., Qi, Y.Q., Wang, T., Coulson, I.M., 2008b. Zircon U–Pb geochronology and major, trace elemental and Sr–Nd–Pb isotopic geochemistry of mafic dykes in western Shandong Province, east China: constraints on their petrogenesis and geodynamic significance. Chem. Geol. 255, 329–345.
Liu, S., Hu, R.Z., Feng, G.Y., Yang, Y.H., Feng, C.X., Qi, Y.Q., Wang, T., 2010a. Distribution and significance of the mafic dyke swarms since Mesozoic in North China Craton. Geol. Bull. China 29, 1–9.
Liu, Y.S., Gao, S., Hu, Z., Gao, C., Zong, K., Wang, D., 2010b. Continental and oceanic crust recycling-induced melt–peridotite interactions in the Trans-North China Orogen: U–Pb dating: Hf isotopes and trace elements in zircons of mantle xenoliths. J. Petrol. 51, 537–571.
Liu, Y.S., Hu, Z.C., Zong, K.Q., Gao, C.G., Gao, S., Xu, J., Chen, H.H., 2010c. Reappraisement and refinement of zircon U–Pb isotope and trace element analyses by LA-ICP-MS. Chin. Sci. Bull. 55, 1535–1546.
Ludwig, K.R., 2003. ISOPLOT 3.00: A Geochronological Toolkit for Microsoft Excel: Berkeley. Geochronology Center, California.
Lugmair, G.W., Harti, K., 1978. Lunar initial $^{143}Nd/^{144}Nd$: differential evolution of the lunar crust and mantle. Earth Planet. Sci. Lett. 39, 349–357.
Ma, Q., Zheng, J.P., 2009. In-situ U–Pb dating and Hf isotopic analyses of zircon in the volcanic rock of the Lanqi formation in the Beipiao area, western Liaoning Province. Acta Petrol. Sinica 25, 3287–3297.
Maruyama, S., Seno, T., 1986. Orogeny and relative plate motions: example of the Japanese Islands. Tectonophysics 127, 306–329.
Maruyama, S., Isozaki, Y., Kimura, G., Terabayashi, M., 1997. Paleographic maps of the Japanese Islands: plate tectonic synthesis from 750 Ma to the present. Island Arc 6, 121–142.
Miyashiro, A., 1973. Metamorphism and Metamorphic Belts. George Allen & Unwin, London, pp. 1–492.
Mohr, P.A., 1987. Crustal contamination in mafic sheets: a summary. In: Halls, H.C., Fahrig, W.C. (Eds.), Mafic Dyke Swarms, vol. 34. Special Publication-Geological Association of Canada, pp. 75–80.
Niu, M.L., 2001. Magmatic Activities and Deep Processes in the Middle-Southern Part of the Tan-Lu Fault Zone (Doctoral Degree Thesis). Hefei University of Technology, Hefei.
Peng, Z.C., Zartman, R.E., Futa, K., Chen, D.G., 1986. Pb-isotopic, Sr-isotopic and Nd isotopic systematics and chemical characteristics of Cenozoic basalts, eastern China. Chem. Geol. 59, 3–33.
Potts, P.J., Kane, J.S., 2005. International association of geoanalysts certificate of analysis: certified reference material OU-6 (Penrhyn slate). Geostandards Geoanal. Res. 29, 233–236.
Qi, L., Conrad, G.D., 2000. Determination of trace elements in twenty six Chinese geochemistry reference materials by inductively coupled plasma-mass spectrometry. J. Geostandards Geoanal. 24, 51–63.
Shao, J.A., Liu, F.T., Chen, H., Han, Q.J., 2001. Relationship between Mesozoic magmatism and subduction in Da Hinggan-Yanshan area. Acta Geol. Sinica 75, 56–63.
Song, X.Y., Qi, H.W., Robinson, P.T., Zhou, M.F., Cao, Z.M., Chen, L.M., 2008. Melting of the subcontinental lithospheric mantle by the Emeishan mantle plume; evidence from the basal alkaline basalts in Dongchuan, Yunnan, Southwestern China. Lithos 100, 93–111.
Steiger, R.H., Jäger, E., 1977. Subcommission on Geochronology: convention on the use of decay constants in geochronology and cosmochronology. Earth Planet. Sci. Lett. 36, 359–362.
Sun, S.S., McDonough, W.F., 1989. Chemical and isotopic systematics of o c e a nic basalts: implications for mantle composition and processes. In: Saunders, A.D., Norry, M.J. (Eds.), Magmatism in the Ocean Basins, vol. 42. Geological Society London Special Publication, pp. 313–345.
Thompson, M., Potts, P.J., Kane, J.S., Wilson, S., 2000. An international proficiency test for analytical geochemistry laboratories-report on round 5 (august 1999). Geostandards Geoanaly. Res. 24, 1–28.
Wang, D.Z., Ren, Q.J., Qiu, J.S., Chen, K.R., Xu, Z.W., Zen, J.H., 1996. Characteristics of volcanic rocks in the shoshonite province, eastern China, and their metallogenesis. Acta Geol. Sinica 70, 23–34.
Wang, X., Griffin, W.L., Wang, Z., Zhou, X.M., 2003. Hf isotope compositions of zircons and implications for the petrogenesis of Yajiangqiao granite, Hunan Province, China. Chin. Sci. Bull. 48, 995–998.
Wiedenbeck, M., Alle, P., Corfu, F., Griffin, W.L., Meier, M., Oberli, F., Quadt, A.V., Roddick, J.C., Spiegel, W., 1995. Three natural zircon standards for U–Th–Pb, Lu–Hf, trace element and REE analyses. Geostandards Geoanaly. Res. 19, 1–23.
Wilde, S.A., Zhao, G.C., Sun, M., 2002. Late Archaean to Early Palaeoproterozoic magmatic events in the North China Craton: the prelude to amalgamation. Gondwana Res. 5, 85–94.
Wilde, S.A., Wu, F.Y., Zhao, G.C., 2010. The Khanka Block, NE China, and its significance for the evolution of the Central Asian Orogenic Belt and continental accretion. Geol. Soc. London Special Publ. 338, 117–137.
Windley, B.F., 1984. The Evolving Continents. John Wiley & Sons, p. 420.
Wu, L.R., 1985. Mesozoic granitoids in east China. Acta Petrol. Sinica 1, 1–10.
Wu, F.Y., Jahn, B.M., Lin, Q., 1997. Isotopic characteristics of the post-orogenic granites in the orogenic belt of Northern China and their implications for crustal growth. Chin. Sci. Bull. 42, 2188–2191.
Wu, F.Y., Jahn, B.M., Wilde, S.A., Sun, D.Y., 2000. Phanerozoic continental crustal growth: U–Pb and Sr–Nd isotopic evidence from the granites in northeastern China. Tectonophysics 328, 89–113.
Wu, F.Y., Ge, W.C., Sun, D.Y., Guo, C.L., 2003a. Discussions on the lithospheric thinning in eastern China. Earth Sci. Front. 10, 51–60.
Wu, F.Y., Walker, R.J., Ren, X.W., Sun, D.Y., Zhou, X.H., 2003b. Osmium isotopic constraints on the age of lithospheric mantle beneath northeastern China. Chem. Geol. 197, 107–129.
Wu, F.Y., Lin, J.Q., Wilde, S.A., Sun, D.Y., Yang, J.H., 2005a. Nature and significance of the Early Cretaceous giant igneous event in eastern China. Earth Planet. Sci. Lett. 233, 103–119.
Wu, F.Y., Yang, J.H., Wilde, S.A., Zhang, X.O., 2005b. Geochronology, petrogenesis and tectonic implications of the Jurassic granites in the Liaodong Peninsula, NE China. Chem. Geol. 221, 127–156.
Wu, F.Y., Xu, Y.G., Gao, S., Zheng, J.P., 2008. Lithospheric thinning and destruction of the North China Craton. Acta Petrol. Sinica 24, 1145–1174.
Wu, F.Y., Sun, D.Y., Ge, W.C., Zhang, Y.B., Matthew, L., Grant, Wilde, S.A., Jahn, B.M., 2011. Geochronology of the Phanerozoic granitoids in northeastern China. J. Asian Earth Sci. 41, 1–30.
Xiao, Y., Zhang, H.F., Fan, W.M., Ying, J.F., Zhang, J., Zhao, X.M., Su, B.X., 2010. Evolution of lithospheric mantle beneath the Tan-Lu fault zone, eastern North China Craton: evidence from petrology and geochemistry of peridotite xenoliths. Lithos 117, 229–246.
Xu, Y.G., 2001. Thermo-tectonic destruction of the Archean lithospheric keel beneath the Sino-Korean craton in China: evidence, timing and mechanism. Phys. Chem. Earth (A) 26, 747–757.
Xu, J.W., Zhu, G., Tong, W.X., Cui, K.R., Liu, Q., 1987. Formation and evolution of the Tancheng-Lujiang wrench fault system: a major shear system to the northwest of the Pacific Ocean. Tectonophysics 134, 273–310.
Xu, Y.G., Ross, J.V., Mercier, J.C.C., 1993. The upper-mantle beneath the continental rift of Tan-Lu, eastern China-evidence for the intra-lithospheric shear zones. Tectonophysics 225, 337–360.

Xu, Y.G., Menzies, M.A., Mattey, D.P., Lowry, D., Harte, B., Hinton, R.W., 1996. The nature of the lithospheric mantle near the Tancheng-Lujiang fault, China: an integration of texture, chemistry and O-isotopes. Chem. Geol. 134, 67–81.

Xu, W.L., Wang, Q.H., Wang, D.Y., Pei, F.P., Gao, S., 2004. Processes and mechanism of Mesozoic lithospheric thinning in eastern North China Craton: evidence from Mesozoic igneous rocks and deep-seated xenoliths. Earth Sci. Front. 11, 309–317.

Yan, G.H., Mu, B.L., Xu, B.L., 2000. Geochronology and Sr–Nd–Pb isotopic characteristics and significance of the Triassic alkaline intrusions from the Yanliao-Yinshan area. Sci. China (D) 30, 383–387.

Yang, W., 2007. Geochronology and geochemistry of the Mesozoic volcanic rocks in Western Liaoning: constraints on the mechanism of lithospheric thinning in the North China Craton. PhD. Thesis, University of Science and Technology of China.

Yang, W., Li, S.G., 2008. Geochronology and geochemistry of the Mesozoic volcanic rocks in Western Liaoning: implications for lithospheric thinning of the North China Craton. Lithos 102, 88–117.

Zhai, M.G., 2008a. State of lithosphere beneath the North China Craton before the Mesozoic lithospheric disruption: a suggestion. Geotectonica et Metallogenia 32, 516–520.

Zhai, M.G., 2008b. Lower crust and lithospheric mantle beneath the North China Craton before the Mesozoic lithospheric disruption. Acta Petrol. Sinica 24, 2185–2204.

Zhai, M.G., Fan, H.R., Yang, J.H., Miao, L.C., 2004. Large scale cluster of gold deposits in east Shandong: Anorogenic metallogenesis. Earth Science Frontiers (China University of Geosciences, Beijing) 11, 85–97.

Zhang, G.R., 2006. Mesozoic intraplate orogenesis in western Liaoning Province, China. Ph.D. Thesis, China University of Geosciences (Beijing).

Zhang, H.F., Sun, M., Zhou, X.H., Fan, W.M., Zhai, M.G., Yin, J.F., 2002. Mesozoic lithosphere destruction beneath the North China Craton: evidence from major, trace element and Sr–Nd–Pb isotope studies of Fangcheng basalts. Contrib. Mineral. Petrol. 144, 241–253.

Zhang, H.F., Sun, M., Zhou, M.F., Fan, W.M., Zheng, J.P., 2003. Secular evolution of the lithosphere beneath the eastern North China Craton: evolution from Mesozoic basalts and high-Mg andesites. Geochimica et Cosmochimica Acta 67, 4373–4387.

Zhang, H.F., Sun, M., Zhou, M.F., 2004. Highly heterogeneous Late Mesozoic lithospheric mantle beneath the North China Craton: evidence from Sr–Nd–Pb isotopic systematic of mafic igneous rocks. Geol. Mag. 141, 55–62.

Zhang, H., Liu, X.M., Chen, W., Li, Z.T., Yang, F.L., 2005a. The age of the top of the Yixian Formation in the Beipiao-Yixian area, western Liaoning, and its importance. Geol. China 32, 596–603.

Zhang, H.F., Sun, M., Zhou, X.H., Ying, J.F., 2005b. Geochemical constraints on the origin of Mesozoic alkaline intrusive complexes from the North China Craton and tectonic implications. Lithos 81, 297–317.

Zhang, S.H., Zhao, Y., Song, B., Yang, Z.Y., Hu, J.M., Wu, H., 2007. Carboniferous granitic plutons from the northern margin of the North China block: implications for a Late Paleozoic active continental margin. J. Geol. Soc. London 164, 451–463.

Zhao, G.C., 2001. Paleoproterozoic assembly of the North China Craton. Geol. Mag. 138, 87–91.

Zhao, G.C., Cawood, P.A., 2012. Precambrian Geology of China. Precambrian Res. 222–223, 13–54.

Zhao, G.C., Zhai, M.G., 2013. Lithotectonic elements of Precambrian basement in the North China Craton: review and tectonic implications. Gondwana Res. 23, 1207–1240.

Zhao, H.L., Deng, J.F., Chen, F.J., Hu, Q., Zhao, S.K., 1998. The basin formation in northeast China. Geoscience 12, 56–62.

Zhao, G.C., Wilde, S.A., Cawood, P.A., Sun, M., 2001. Archean blocks and their boundaries in the North China Craton: lithological, geochemical, structural and P–T path constraints and tectonic evolution. Precambrian Res. 107, 45–73.

Zhao, G.C., Sun, M., Wilde, S.A., Li, S.Z., 2005. Late Archean to Paleoproterozoic evolution of the North China Craton: key issues revisited. Precambrian Res. 136, 177–202.

Zheng, Y.F., Wu, F.Y., 2009. Growth and reworking of cratonic lithosphere. Chin. Sci. Bull. 54, 3347–3353.

Zheng, J.P., O'Reilly, S.Y., Griffin, W.L., Lu, F.X., Zhang, M., 1998. Nature and evolution of Cenozoic lithospheric mantle beneath Shandong peninsula, Sino-Korean Craton, eastern China. Int. Geol. Rev. 40, 471–499.

Zheng, J.P., Griffin, W.L., O'Reilly, S.Y., Yu, C.M., Zhang, H.F., Pearson, N., Zhang, M., 2007. Mechanism and timing of lithospheric modification and replacement beneath the eastern North China Craton: peridotitic xenoliths from the 100 Ma Fuxin basalts and a regional synthesis. Geochimica et Cosmochimica Acta 71, 5203–5225.

Zhou, X.H., 2006. Major transformation of subcontinental lithosphere beneath eastern China in the Cenozoic-Mesozoic: review and prospect. Earth Sci. Front. 13, 50–54.

Zhou, D.W., Zhang, C.L., Liu, Y.Y., 1998. Study on basic dyke swarms developed in the basement in the continental orogen: an example from Wudang block in Southern Qinling. Adv. Earth Sci. 13, 151–156.

Zhou, X.H., Zhang, G.H., Yang, J.H., Chen, W.J., Sun, M., 2001. Sr–Nd–Pb isotope mapping of late Mesozoic volcanic rocks across the northern margin of the North China Craton and implications to geodynamic processes. Geochimica 30, 10–23.

Zhou, X.H., Zhang, H.F., Ying, J.F., Chen, L.H., 2005. Geochemical records of subsequent effects of continental deep subduction: discussion of mantle source variations of the Mesozoic lithospheric mantle of the North China Craton. Acta Petrol. Sinica 21, 1255–1264.

Zhou, J.B., Wilde, S.A., Zhang, X.Z., Zhao, G.C., Zheng, C.Q., Wang, Y.J., Zhang, X.H., 2009. The onset of Pacific margin accretion in NE China: evidence from the Heilongjiang high-pressure metamorphic belt. Tectonophysics 478, 230–246.

Zhou, J.B., Wilde, S.A., Zhao, G.C., Zhang, X.Z., Zheng, C.Q., Wang, H., 2010a. Pan-African metamorphic and magmatic rocks of the Khanka Massif, NE China: further evidence regarding their affinity. Geol. Mag. 147, 737–749.

Zhou, J.B., Wilde, S.A., Zhao, G.C., Zhang, X.Z., Zheng, C.Q., Wang, H., Zeng, W.S., 2010b. An intriguing dilemma: was the easternmost segment of the central asian orogenic belt derived from Gondwana. J. Geodyn. 50, 300–317.

Zhou, J.B., Wilde, S.A., Zhao, G.C., Zhang, X.Z., Zheng, C.Q., Wang, H., 2010c. New SHRIMP U–Pb zircon ages from the Heilongjiang high-pressure belt: constraints on the Mesozoic evolution of NE China. Am. J. Sci. 310, 1024–1053.

Zhou, J.B., Wilde, S.A., Zhang, X.Z., Zhao, G.C., Liu, F.L., Qiao, D.W., Ren, S.M., Liu, J.H., 2011. A > 1300 km late Pan-African metamorphic belt in NE China: new evidence from the Xing'an block and its tectonic implications. Tectonophysics 509, 280–292.

Zhu, R.X., Zheng, T.Y., 2009. Destruction geodynamics of the North China Craton and its Paleoproterozoic plate tectonics. Chin. Sci. Bull. 54, 3354–3366.

Zhu, G., Song, C.Z., Wang, D.X., Liu, G.S., Xu, J.W., 2001a. Studies on ^{40}Ar–^{39}Ar thermochronology of strike-slip time of the Tan-Lu fault zone and their tectonic implications. Sci. China (Series D) 44, 1002–1009.

Zhu, G., Wang, D.X., Liu, G.S., Song, C.Z., Xu, J.W., Niu, M.L., 2001b. Extensional activities along the Tan-Lu fault zone and its geodynamic setting. Chin. J. Geol. 36, 269–278.